First-Principles Investigation of Low Energy E^{′} Center Precursors in Amorphous Silica

Nathan L. Anderson, Ravi Pramod Vedula, Peter A. Schultz, R. M. Van Ginhoven, and Alejandro Strachan

Phys. Rev. Lett. **106**, 206402 — Published 17 May 2011

DOI: 10.1103/PhysRevLett.106.206402

First-Principles Investigation of Low Energy E′ Center Precursors in Amorphous Silica

Nathan L. Anderson,[1] Ravi Pramod Vedula[2], Peter A. Schultz,[3] R.M. Van Ginhoven,[4] and Alejandro Strachan.[1]

[1]*School of Materials Engineering, Purdue University, West Lafayette, Indiana*

[2]*School of Electrical and Computer Engineering, Purdue University, West Lafayette, Indiana*

[3]*Sandia National Laboratories, Albuquerque, New Mexico*

[4]*Pacific Northwest National Laboratory, Richland, Washington*

We show that oxygen vacancies are not necessary for the formation of E' centers in amorphous SiO_2 and that a single O-deficiency can lead to two charge traps. Employing molecular dynamics with a reactive potential and density functional theory we generate an ensemble of stoichiometric and oxygen-deficient amorphous SiO_2 atomic structures and identify low-energy network defects. Three-coordinated Si atoms appear in several low-energy defects both in stoichiometric and O-deficient samples where, in addition to the neutral oxygen vacancy, they appear as isolated defects.

Amorphous silicon dioxide (a-SiO_2) is important in many technological applications, from microelectronics to optical transmission media. Whether generated by manufacturing, irradiation, or even mechanical deformation, defects capable of trapping charge in a-SiO_2 are responsible for degrading device performance, leading to threshold voltage shifts in metal-oxide-semiconductor transistors, actuation voltage changes in micro-electromechanical systems (MEMS) and attenuation in optical fibers. The experimentally observed families of E′ centers are associated with trapping charge and are believed to play an important role in this degradation [1,2].

The correlation between three-coordinated Si precursors (III-Si) and E' centers in silica is firmly established, with electronic structure calculations on proposed atomic models [1,2] predicting spectroscopic features in good

agreement with electron paramagnetic resonance (EPR) experiments [3,4]. However, significant challenges remain; the high concentration of E' centers observed experimentally in stoichiometric *a*-SiO_2, see for example Ref. [5], cannot be explained by current models of *a*-SiO_2, all of which assume an oxygen vacancy to be the origin of the defects. Besides their local coordination, definitive structural models for these defects remain debatable, as does their formation under differing glass forming conditions. Using a combination of molecular dynamics (MD) and density functional theory (DFT), we predict that III-Si precursor centers occur as part of several low-energy defects both in oxygen-deficient and stoichiometrically perfect *a*-SiO_2 samples, showing that an oxygen vacancy is not necessary to form E' centers in *a*-SiO_2 (similar to findings in α–Quartz by Boero *et al.* [6]).

The commonly proposed E'_γ and E'_δ precursor in *a*-SiO_2 is a neutral oxygen vacancy (NOV), a missing O atom that leaves behind a Si-Si pair. Theoretical calculations have shown that an EPR-active center occurs when one of the silicon atoms retreats from the oxygen vacant site and becomes tetrahedrally coordinated with another oxygen atom in the amorphous network, known as the puckered configuration [3]. The resulting structure leaves an unpaired electron spin localized on a single silicon sp^3 hybrid orbital and has spectroscopic signals consistent with the EPR experiments on the E'_γ center. Electronic structure calculations have also shown that if the Si-Si bond in a NOV captures a hole and remains a dimer, the resulting properties agree well with the E'_δ EPR signals [3,4]; this time the unpaired electron spin is delocalized over a pair of silicon sp^3 hybrid orbitals. Our calculations predict the NOV to be a common defect in oxygen deficient samples but, more interestingly, that isolated III-Si atoms appear in several common native defects. This indicates the presence of a more direct precursor to the E'_γ center than the NOV in both oxygen deficient and stoichiometric samples.

One of the key factors hindering progress in this field is that the prediction of well-equilibrated atomic structures representative of amorphous materials remains a significant computational challenge. It requires both an accurate atomistic description of configurational energies, including defects, and an extensive exploration of

configuration space to avoid getting trapped in unphysical high-energy structures, as often occurs with fast quenches. To address this challenge, we combine MD simulations using the reactive potential ReaxFF with a slow annealing procedure designed to minimize artifacts seen in previous studies, followed by energy minimization using DFT to refine the candidate amorphous models and obtain their energies. The ReaxFF force field we use is based on *ab initio* calculations of silicon and silica [7] including the equation of state of various phases as well as the structure and energetics of small molecules. The MD simulations are performed with a Berendsen thermostat and barostat with coupling constants of 10 fs and 5000 fs, respectively. The DFT calculations use SeqQuest[8], in the generalized gradient approximation by Perdew, Burke, and Ernzerhof (GGA-PBE) [9] with Troullier-Martins pseudopotentials [10] for oxygen and a Hamann pseudopotential [11] for silicon, and double-zeta plus polarization basis sets. The Γ-point was adequate for Brillouin-zone integration for the large supercells used in the amorphous models [12]. Additional simulation details are described in the supplementary material together with the ReaxFF force field parameter file [12].

Initial structures with 72 and 192 atoms were generated by replicating the 9-atom trigonal α–quartz and 24-atom β-cristobalite unit cells twice along each cell vector and transforming the resulting structures into orthogonal cells. We then performed 5 independent 1,500 ps long MD simulations for each supercell at 4000 K and a density of 2.3 g/cm^3 (atmospheric pressure) to melt and randomize the structures. From each MD run we selected 12 independent liquid configurations, the first at 400 ps and one every 100 ps thereafter, for a total of 60 well equilibrated, stoichiometric liquid samples for each cell size. We generated 60 oxygen deficient samples for each size repeating the procedure above, first removing one oxygen atom at random from each initial structure prior to the T=4000K liquid runs. Each sample, stoichiometric and oxygen-deficient, was then slowly annealed from 4000K to 300K under isobaric conditions at a rate of 1.67 K/ps. This rate is slower than those used in previous studies [13,14], and results in well-annealed a-SiO_2 structures with a lower incidence of unphysical network artifacts. All samples were treated as neutral, with no net charge.

Each resulting amorphous structure (60 stoichiometrically perfect and 60 oxygen deficient for each size) was relaxed using DFT energy minimization with respect to atomic positions. The average density of the cells (predicted by ReaxFF) 2.22±0.18 g/cm^3 is in good agreement with the experimental values of 2.20 g/cm^3 (applicable to high purity fused silica used in optical fibers [15]), and 2.23-2.27 (applicable to thermally oxidized silica used in MOSFET devices [16]). Finally, a structural analysis was performed to identify and classify the structures and their defects. A defect-free *a*-SiO2 structure is defined as a continuous random network of SiO_4 tetrahedra with two-fold coordinated oxygen atoms bridging tetrahedrally coordinated Si. To identify defects, we calculate the coordination number of every atom using a bond cutoff of 2 Å. For the stoichiometric samples, 75% and 37% of the 72- and 192-atom cells are defect-free, respectively. Most of the remaining stoichiometric cells exhibit a single isolated defect or defect pair. For the oxygen deficient samples, 97% of the 71-atom cells and 70% of the 191-atom cells contain only a single isolated defect or minimum defect pair needed to accommodate a missing oxygen atom. All 240 structures obtained together with a description of their defects are available electronically as supplementary material [12].

Figs. 1 and 2 show typical atomic configurations of defects in stoichiometric and oxygen deficient *a*-SiO_2 respectively; Fig. 3 (b-f) shows the distributions of formation energies of each defect type. All energies quoted here correspond to DFT relaxed structures for the 192- and 191-atom systems at T=0 K (zero point energy is not taken into account). The smaller cells yield similar defect energies, shown in the supplementary material [12]. It is important to note the large variations in defect formation energy, see Fig. 3, due to the amorphous nature of the structures. As was discussed in Ref. [17] this underscores the importance of generating and analyzing ensembles of representative structures as opposed to drawing conclusions from a single calculation.

Defect formation energies are presented with respect to amorphous silica in the oxygen rich limit. The amorphous silica reference cell energy, $E_{a\text{-}SiO2}$, is taken to be the average energy of all defect-free stoichiometric samples (see Fig. 3(a)), and the oxygen reference E_{O_2} is the energy of a spin-polarized DFT calculation of an

oxygen molecule in the triplet ground state. The formation energy (E_f) for the defects in oxygen deficient samples is obtained from the energy of the defective sample (E^{def}_{a-SiO2}), E_{O_2} , and $E_{a\text{-}SiO2}$:

$$E_f = E^{def}_{a-SiO2} + \frac{1}{2}E_{O_2} - E_{a-SiO2} \quad (1)$$

The defect formation energies in the Si-rich limit (given in the supplementary material [12] can be obtained from the O-rich values using the computed heat of formation of α–quartz from diamond Si and O_2 (8.12 eV/SiO_2) and the computed heat of amorphization to form a-SiO_2 from α–quartz (0.23 eV/SiO_2).

The most common defects observed in stoichiometric samples are: i) a pair of three-fold and five-fold coordinated Si atoms (III-Si/V-Si), Fig. 1(a), and ii) a three-fold oxygen and five-fold silicon pair (III-O/V-Si), Fig. 1(b). The III-Si/V-Si has the lowest formation energy of all reported defects at about 1.7 eV (Fig. 3(b)). This is a surprisingly low energy, similar to the amorphization energy of only 8 SiO_2 formula units. Three- and five-fold Si have been reported in previous simulations [13,17]—fast cooling rates in MD simulation tend to artificially trap large numbers of these defects—however, their formation energy has not been reported. Their appearance as isolated defect pairs in our simulations with slower cooling rates and low formation energies indicate that III-Si and V-Si are likely a native defects in a-SiO_2. Five-fold silicon atoms, V-Si, in a-SiO_2 have been tentatively identified in solid-state nuclear magnetic resonance studies [18], thus suggesting the existence of a compensating companion III-Si, a direct precursor to E'_γ centers. The second important defect found in stoichiometric systems is the III-O/V-Si pair with formation energy about 0.5 eV higher than the III-Si/V-Si (Fig. 3(c)). Overcoordinated oxygen has been observed in prior MD and DFT studies of vitreous silica and has been hypothesized to play a significant role allowing the amorphous network to generate during silicon oxidation [19]. Our DFT calculations show the III-O to form approximately planar structures with three Si-O bonds that are, in average, 0.2Å longer than those among perfectly coordinated Si and O atoms. The III-O, just as overcoordinated O atoms bonding with hydrogen [20], may trap holes and III-O atoms have been hypothesized in aluminosilicate glasses to explain NMR [21].

We now turn our attention to oxygen-deficient samples. As expected from prior studies, the NOV is frequently observed in these samples; shown in Fig. 2(a) this defect is the typically assumed precursor for E'$_\gamma$ and E'$_\delta$ centers. Previous DFT-LDA calculations have reported the average NOV formation energy as 5.6 eV [22] (O-rich limit), which significantly higher than our average value of 4.4 eV, see Fig. 3(d). This is likely a product of strain relaxation with some influence from the different choice of functional; each simulation cell in our work is annealed with a missing oxygen from the melt and relaxed, as opposed to annealing a stoichiometric sample and then removing a network oxygen.

A more interesting defect to emerge from these oxygen-deficient simulations is a pair of dissociated three-fold silicon atoms (D-III-Si), see Fig. 2(b). This defect can be described as a dissociated oxygen vacancy; the two three-fold silicon atoms in the D-III-Si pair do not share an oxygen vacancy site (as in the NOV). Each of the two III-Si defects is a more direct structural precursor to an E′$_\gamma$ center than the NOV, it does not require a Si atom to pucker away from a dimer configuration. Furthermore, both undercoordinated Si atoms are E'$_\gamma$ precursors, leading to two charge traps per oxygen deficiency. While the average formation energy of the dissociated III-Si pair is ~1.5 eV (Fig. 3(e)) higher than of the NOV, it is entropically favored since the location of the two Si atoms need not be correlated. In our simulations both defects appear with very similar probabilities (17% for NOV and 18% for D-III-Si). This indicates that isolated III-Si are likely common defects in oxygen deficient *a*-SiO_2.

Another common defect observed in the oxygen-deficient samples has an overcoordinated oxygen and an undercoordinated silicon (III-O/III-Si), see Figs. 2(c) and 3(f). This pair of defects again yields a possible E' precursor with the III-Si, and the appearance of III-O is analogous to the III-O/V-Si defect observed in stoichiometric samples. Finally, three of the oxygen-deficient samples contained an isolated divalent silicon (II-Si) with average formation energy of 3.0 eV. This defect, denoted ODC(II) in the past, is shown in Fig. 2(d) has

been attributed an optical absorption peak in luminescence polarization experiments [2]. The II-Si has been hypothesized as a precursor to other types of E' centers [1].

It is interesting to note that III-O/V-Si and III-Si/V-Si defects in stoichiometric samples have average formation energies within an electron volt, as do the D-III-Si and III-O/III-Si defects in oxygen deficient samples. This indicates that formation energy of the III-O is fairly close to the III-Si, and that these defects may be present in a-SiO_2 in comparable concentrations.

In summary, we used MD simulations with an accurate reactive force field and DFT calculations to identify non-vacancy network defects in *a*-SiO_2 that can act as precursors to E' centers. We have shown that III-Si atoms, known precursors to E′ centers, are low-energy defects not only in O-deficient environments but also in samples with perfect stoichiometry down to the ~$(1.5\ nm)^3$ scale, which provides a plausible explanation for the unexplained abundance of E' centers observed experimentally in stoichiometric *a*-SiO_2 [5]. Furthermore, we find that in oxygen deficient cases III-Si atoms appear not only as NOV's but also as dissociated defects, and yield two E' precursors per oxygen deficiency. We also find that overcoordinated O atoms are low energy defects both in stoichiometric and oxygen deficient samples; these defects can also play an important role in charge trapping. These low-energy defects and defect pairs emerge directly from well-equilibrated samples obtained via unbiased MD simulations from the melt, rather than from assumptions in the construction of the model. This statistical relaxed-defect approach is generally applicable to a wide range of amorphous materials including those for which little is known about possible defects and to explore new materials where no experimental data is available. The accuracy and reliability of the predictions depends on analysis of an extensive ensemble of structural models generated by MD simulations that contains a statistically meaningful sampling of the dominant defects. This requires fast and accurate interatomic MD potentials and quenching rates slow enough to avoid freezing in high energy artifacts.

The authors thank Harold P. Hjalmarson and Arthur H. Edwards for useful discussions. This work was partly supported by Purdue's Center for the Prediction of Reliability, Integrity and Survivability of Microsystems (PRISM) funded by the US Department of Energy's National Nuclear Security Administration under contract Award No. DE-FC52-08NA28617. Computational resources of NSF's Network for Computational Nanotechnology and nanoHUB.org are gratefully acknowledged. Sandia National Laboratories is a multi-program laboratory operated by Sandia Corporation, a wholly owned subsidiary of Lockheed Martin company, for the U.S. Department of Energy's National Nuclear Security Administration under contract DE-AC04-94AL85000.

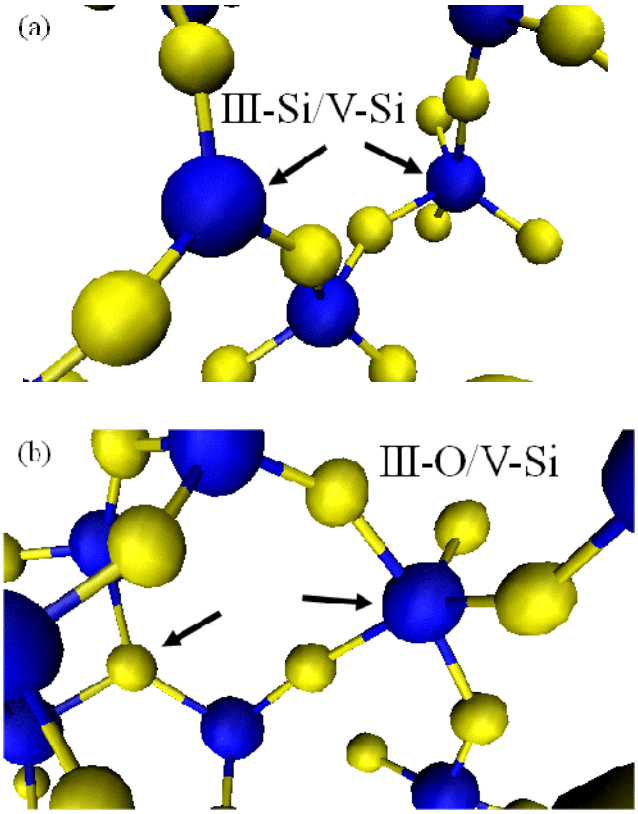

FIG. 1. Defects in stoichiometric samples. (a) a pair of three-fold and five-fold coordinated silicon atoms (III-Si/V-Si). The undercoordinated silicon has a dangling bond and could be a precursor to the E'_γ center without an oxygen vacancy. The low formation energy suggests that this is likely a native defect in *a*-SiO_2. (b) a pair of 3-coordinated oxygen and 5-coordinated silicon atoms (III-O/V-Si). We find that III-O forms with a formation energy ~0.5 eV higher than III-Si.

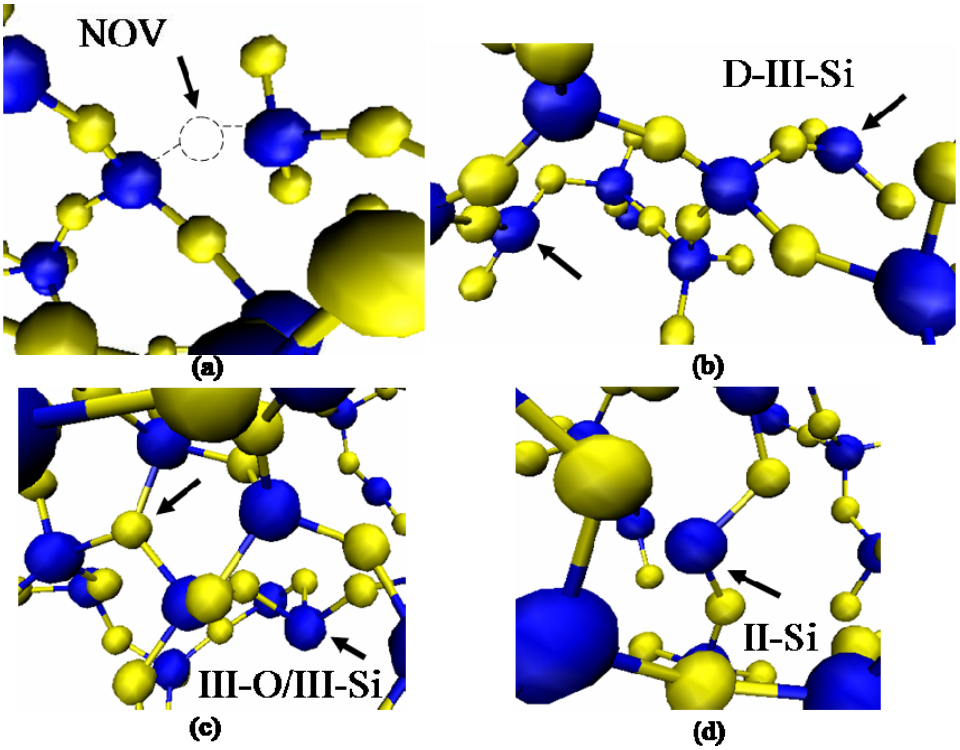

FIG. 2. Defects in oxygen deficient samples. (a) a neutral oxygen vacancy (NOV) in which two silicon atoms share a missing oxygen site and usually forming a Si-Si bond, this is the typically assumed E' precursor. (b) Two dissociated 3-coordinated silicon atoms (D-III-Si), the Si atoms do not share a single oxygen vacancy site resulting in two more direct E'_{γ} precursors than the NOV. (d) A 3-coordinated oxygen and 3-coordinated silicon pair (III-O/III-Si), the III-Si is a E'_{γ} precursor and the III-O occurs with formation energy ~0.7 eV higher than the III-Si. (d) a two-fold coordinated silicon atom (II-Si), hypothesized as a precursor to an E'_{α} center.

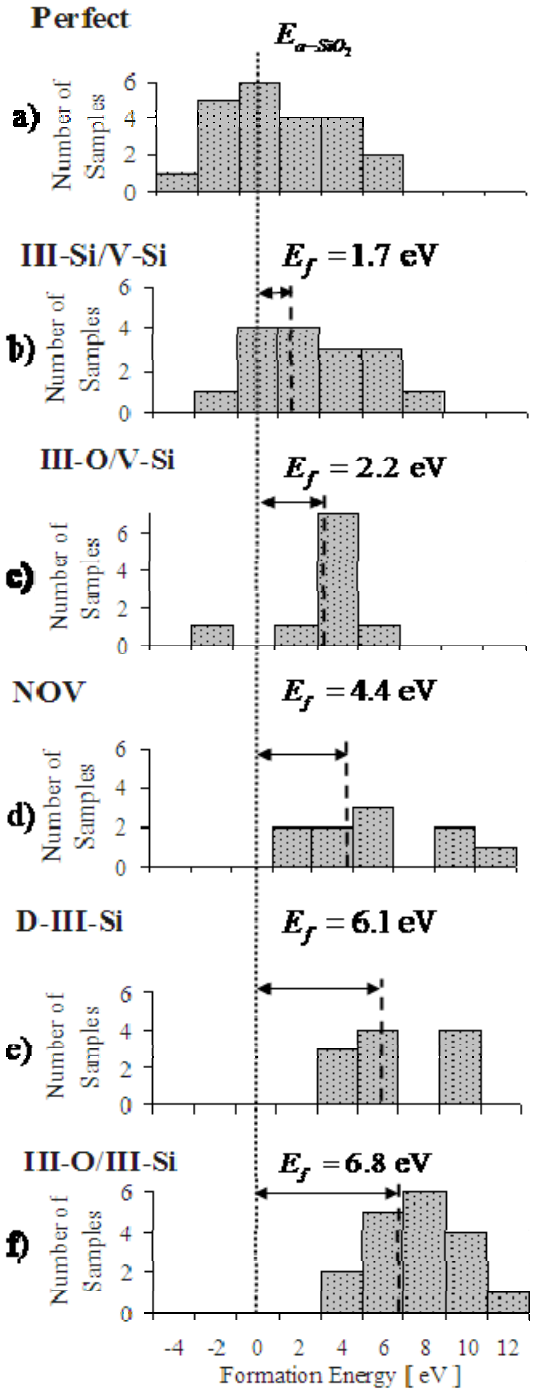

FIG. 3. Histograms of defect formation energies. The small-dashed line indicates the average energy of *all* defect-free samples ($E_{a\text{-}SiO2}$) and large-dashed lines indicate the average formation energy E_f of each defect. (b) and (c) show data for defects found in the stoichiometric samples, and (d), (e), and (f) for the oxygen-deficient samples.

[1] D. L. Griscom, *Defects in SiO_2 and related dielectrics: Science and technology (NATO Science Series, Series II:Mathematical and Physical Chemistry),* ed G. Pacchioni, L. Skuja, and D. L. Griscom, Kluwer, Dordrecht (2000), pp. 122-128.

[2] L. Skuja, *Defects in SiO_2 and related dielectrics: Science and technology (NATO Science Series, Series II: Mathematical and Physical Chemistry),* ed G. Pacchioni, L. Skuja, and D. L.Griscom, Kluwer, Dordrecht (2000), pp. 94-98.

[3] P. V. Sushko, S. Mukhopadhyay, A. S. Mysovsky, V. B. Sulimov, A. Taga, and A. L. Shluger, J. Phys.: Condens. Matter **17**, S2115 (2005).

[4] J. R. Chavez, S. P. Karna, K. Vanheusden, C. P. Brothers, R. D. Pugh, B. K. Singaraju, W. L. Warren, and R. A. B. Devine, IEEE Transactions on Nuclear Science **44**, 1799 (1997).

[5] H. Nishikawa, R. Nakamura, and Y. Ohki, Phys. Rev. B 48, 2968 (1993).

[6] M. Boero, A. Oshiyama, and P. L. Silvestrelli, Phys. Rev. Lett. **91**, 206401 (2003).

[7] A. C. T. van Duin, A. Strachan, S. Stewman, Q. Zhang, X. Xu, and W. A. Goddard III, J. Phys. Chem. A **107**, 3803 (2003); M. J. Buehler, A. C. T. van Duin, and W. A. Goddard III, Phys. Rev. Lett. **96**, 095505 (2006).

[8] http://dft.sandia.gov/Quest/. The DFT simulations in this paper can be repeated online using the "nanoMATERIALS: SeqQuest-DFT" tool available in nanoHUB.org: https://nanohub.org/resources/3982, DOI: 10254/nanohub-r3982.1.

[9] J. P. Perdew, K. Burke, and M. Ernzerhof, Phys. Rev. Lett. **77**, 3865 (1996).

[10] N. Troullier and J. L. Martins, Phys. Rev. B **43**, 8861 (1991).

[11] D. R. Hamann, unpublished.

[12] Supplementary material can be found in XX

[13] X. L. Yuan and A. N. Cormack, J. Non-Cryst. Solids **283**, 69 (2001).

[14] K. Vollmayr, W. Kob, and K. Binder, Phys. Rev. B **54**, 15808 (1996).

[15] "Physical Constants of Inorganic Compunds," in CRC Handbook of Chemistry and Physics, 91st Edition (Internet Version 2011), W.M. Haynes, ed., CRC Press/Taylor and Francis, Boca Raton, FL.

[16] B.J. Mrstik, V.V. Afanas'ev, A. Stesmans, P.J. McMarr, and R.K. Lawrence, J. Appl. Phys. **85**, 6577 (1999).

[17] R. M. Van Ginhoven, H. Jónsson, and L. R. Corrales, Phys. Rev. B **71**, 024208 (2005).

[18] J. Machacek, O. Gedeon, and M. Liska, Phys. Chem. of Glasses **48**, 345 (2007).

[19] A. Pasquarello, M. S. Hybertsen, R. Car, Nature **396**, 58 (1998).

[20] A. H. Edwards, P. A. Schultz, and H. P. Hjalmarson, Phys. Rev. B **69**, 125318 (2004).

[21] J. F. Stebbins and Z. Xu, Nature **390**, 60 (1997).

[22] L. Martin-Samos, Y. Limoge, N. Richard, J. P. Crocombette, G. Roma, E. Anglada, and E. Artacho, Europhysics Letters **66**, 680 (2004).